Many-body quantum chaos in excitonic spectra from first principles

Daniel Hernangómez-Pérez[1,*] and Rafael A. Molina[2,†]

[1] *CIC nanoGUNE BRTA, Tolosa Hiribidea 76, 20018 San Sebastián, Spain*

[2] *Instituto de Estructura de la Materia IEM-CSIC, Serrano 123, E-28006 Madrid, Spain*

CONTENTS

I. Computational details 2

II. Additional results 2

A. Convergence with the **k**-grid of the BSE diagonalization 2

B. Additional statistical analysis 5

C. Higher order spacing ratios 5

References 9

* d.hernangomez@nanogune.eu

† rafael.molina@csic.es

I. COMPUTATIONAL DETAILS

Computational details. The many-body spectra analyzed in this work was obtained from first-principles GW-Bethe Salpether equation (BSE) calculations reported in Ref. [1]. The electronic structure of each heterobilayer was initially computed using density functional theory (DFT), as implemented in Quantum Espresso [2, 3]. Quasiparticle corrections were subsequently evaluated at the G_0W_0 level, including spin-orbit interaction, and the exciton spectra was computed solving the BSE. These calculations were performed using the BerkeleyGW package [4–6]. Further details regarding the structural models, detailed computational methodology, and convergence parameters can also be found in Ref. [1].

Computational subspace scaling. For the disordered system, the BSE Hamiltonian representative sizes scale from a $24 \times 24 \times 1$ grid yielding 112896 eigenvalues, to a $27 \times 27 \times 1$ grid yielding 142884 eigenvalues, and up to a $30 \times 30 \times 1$ grid yielding 176400 eigenvalues. The largest clean system in a grid $36 \times 36 \times 1$ grid configuration, result in a Hamiltonian size that yields 254016 eigenvalues.

II. ADDITIONAL RESULTS

A. Convergence with the k-grid of the BSE diagonalization

When performing Bethe–Salpeter equation (BSE) numerical diagonalization, a critical parameter which controls the convergence is the (super)cell uniform **k**-point grid, as exciton states are defined as coherent superpositions of electron-hole pairs across the Brillouin zone. The convergence with respect to such grid determines (i) how well that discrete **k**-point sampling resolves the interpolated quasiparticle bands and (ii) how precisely the momentum dependence of the Coulomb interaction is captured. As the **k**-point grid is refined, the exciton energies, oscillator strengths, and optical spectra are expected to converge to stable results. We note also that, practically, convergence tests must be performed for each observable of interest, as excitation energies may converge faster that spectral intensities. In other words, the convergence of each observable is independent from each other.

In Figs. S1-S3, we display the dependence on the **k**-grid sampling in the supercell of the average spacing rations (both the clean and lattice-disordered) heterobilayer and the power

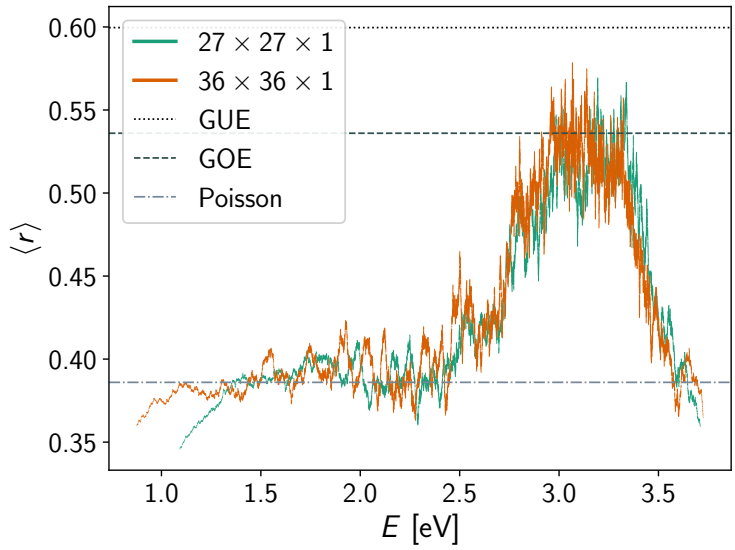

Fig. S1. Average adjacent level spacing ratio, $\langle r \rangle$, taken over windows of 1000 excitonic levels for the pristine WS_2-graphene heterobilayer. We consider two different **k**-grids for the BSE diagonalization. Black dotted, dark grey dashed, and light grey dash-dotted lines denote the theoretical limits for the GUE, GOE, and Poissonian statistics, respectively.

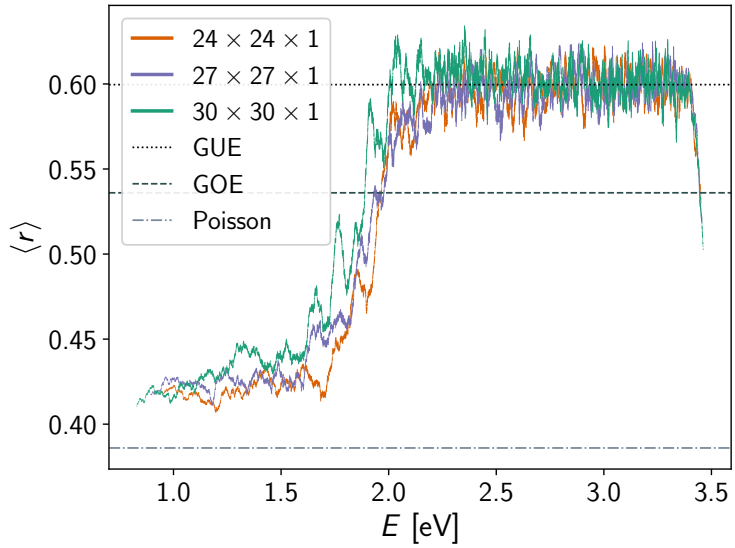

Fig. S2. Average adjacent level spacing ratio, $\langle r \rangle$, taken over windows of 1000 excitonic levels for the WS_2-graphene heterobilayer with lattice disorder. Black dotted, dark grey dashed, and light grey dash-dotted lines denote the theoretical limits for the GUE, GOE, and Poissonian statistics, respectively.

spectrum of the δ_n statistic. All quantities exhibit good quantitative convergence already for the coarsest grid considered, $24 \times 24 \times 1$.

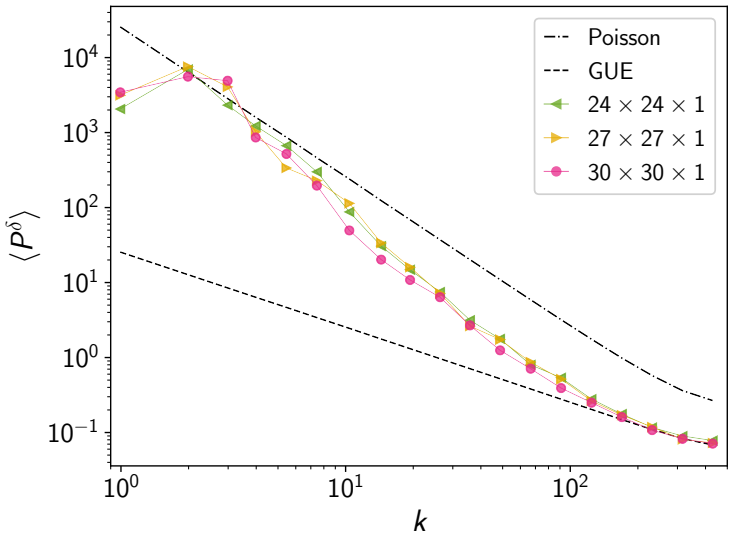

Fig. S3. Dependence of the power spectrum of the δ_n statistic on the **k**-grid employed for the BSE diagonalization. Results are shown for a representative average energy of $\langle E \rangle = 2.39$ eV.

B. Additional statistical analysis

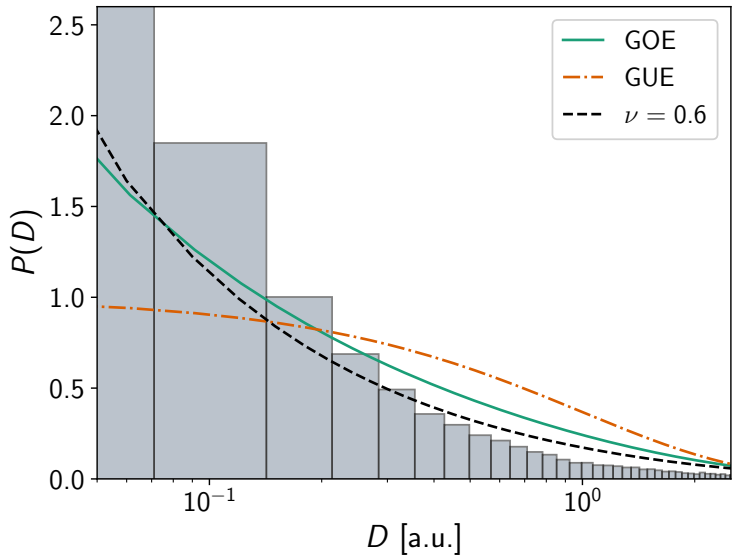

Fig. S4. Histogram of the distribution of the normalized dipolar strength, $D/\langle D\rangle$, for the lattice disordered system in the energy window $E \in [3.15, 3.28]$ eV. We compare our results with a χ^2 distribution with ν degrees of freedom (dashed black line). The case $\nu = 1$ corresponds to the Porter-Thomas distribution for the GUE (dashed dotted orange line), while the GOE result is shown by the solid green line. The horizontal axis is represented in log-scale and only the tail of the distribution and fitting functions are shown.

C. Higher order spacing ratios

Higher–order spacing ratios are a robust tool that can be used to characterize spectral correlations beyond nearest–neighbor level statistics, while retaining the unfolding–free advantage of standard spacing ratios. Given an ordered spectrum defined by the (ordered) ensemble of eigenvalues, $\{E_i\}$, we can define the nearest–neighbor spacings as $s_i = E_{i+1} - E_i$, thus the conventional spacing ratio is given by [7]

$$r_i = \frac{\min\left(s_i, s_{i-1}\right)}{\max\left(s_i, s_{i-1}\right)}. \tag{S1}$$

To generalize this construction, we consider the spacing taken over k levels, $s_i^{(k)} = E_{i+k} - E_i$. Several definitions are now possible, for example, overlapping ratios that probe

correlations at distance of k are given by [8–10]

$$r_i^{(k)} = \frac{\min\left(s_i^{(k)}, s_{i+1}^{(k)}\right)}{\max\left(s_i^{(k)}, s_{i+1}^{(k)}\right)}, \tag{S2}$$

while non-overlapping spacing correlation ratios exploring correlations over $2k$ levels are defined as

$$r_i^{(k)} = \frac{\min\left(s_{i+k}^{(k)}, s_i^{(k)}\right)}{\max\left(s_{i+k}^{(k)}, s_i^{(k)}\right)}. \tag{S3}$$

Note that for $k = 1$ both definitions reduce to the standard next-neighbor ratio in Eq. (S1). Rao [10] has recently study both types of higher-order ratios and shown that non-overlapping definitions are more robust and show a clear universal for random matrix ensembles than overlapping ratios.

These quantities probe correlations at increasingly large spectral scales and are useful for identifying deviations from universal random–matrix behavior, as well as detecting long–range correlations and crossover regimes in which short–range statistics may appear ergodic while longer–range correlations still retain signatures of integrability or localization. However, higher–order spacing ratios present important practical limitations. Since $s_i^{(k)}$ spans k consecutive levels, reliable statistics can only be acquired if the system has sufficiently large spectral windows with an approximately constant density of states. Otherwise, the residual density of state fluctuations can introduce systematic errors analogous to those arising from imperfect unfolding.

In the case of the systems considered here, a transition-metal dichalcogenide-graphene interface, the (many-body) density of states (DoS) is sufficiently large to allow for the computation of non-overlapping spacing ratios up to $k = 5$, enabling a direct comparison with the predictions of the corresponding random-matrix theory (RMT) ensemble. This is mostly due to the nearly continuous single-particle DoS of graphene over a broad region of the relevant single-particle energy spectrum, which enables a large number of allowed optical transitions. To obtain the random matrix theory reference values for each ensemble, we have computed the expectation value of the corresponding higher-order ratio in the central region of the spectrum for large random matrices. We have employed tridiagonal β-Hermite ensemble matrices, which provide an efficient representation for evaluating the ensemble-averaged higher-order ratios with reasonable computational cost [11]. The resulting values

are summarized in Table I.

Table I. Mean higher-order non-overlapping spacing ratios $\langle r^{(k)} \rangle$ for Poisson statistics and the Gaussian random matrix ensembles: orthogonal (GOE), unitary (GUE) and symplectic (GSE). The values for the Gaussian ensemble values for $k > 1$ are numerical estimates.

k	**Poisson**	**GOE**	**GUE**	**GSE**
1	0.3862	0.5300	0.6000	0.6749
2	0.5000	0.6737	0.7306	0.7908
3	0.5620	0.7459	0.7954	0.8432
4	0.6041	0.7909	0.8341	0.8738
5	0.6349	0.8210	0.8594	0.8944

We then plot in Fig. S5 the results of the reduced ratio in order to compare the difference between the result for our system and the RMT result for diferent values of k in the same plot.

We present in Fig. S5 the reduced spacing ratios, defined by

$$\langle \tilde{r}^{(k)} \rangle = \frac{\langle r^{(k)} \rangle - \langle r^{(k)}_{\text{Poisson}} \rangle}{\langle r^{(k)}_{\text{RMT}} \rangle - \langle r^{(k)}_{\text{Poisson}} \rangle}, \tag{S4}$$

to allow for a direct comparison between our the interface results and the corresponding RMT predictions.

These results provide information about the Thouless energy scale of the system as a function of the exciton energy. In particular, the Thouless energy can be estimated from the value of k at which the higher-order spacing start to deviate from the RMT prediction. In the clean case, only the $k = 1$ ratio follows the RMT curve in the energy range between $E \sim 2.9$ eV and $E \sim 3.3$ eV. Therefore, the Thouless energy is of the order of the mean level spacing, $E_{\text{Th}} \sim \Delta E$ within that spectral region. For the lattice disordered case, we find an agreement with the GUE prediction over a substantially broader spectral range. In particular, in the interval $E \in [2.6, 3.3]$ eV, all ratios up to $k = 5$ are compatible with the GUE result, while in the interval $E \in [2.2, 2.6]$ the agreement persists up to $k = 2$. These findings are consistent with the results of long-range correlations obtained from the power spectrum discussed in the main text.

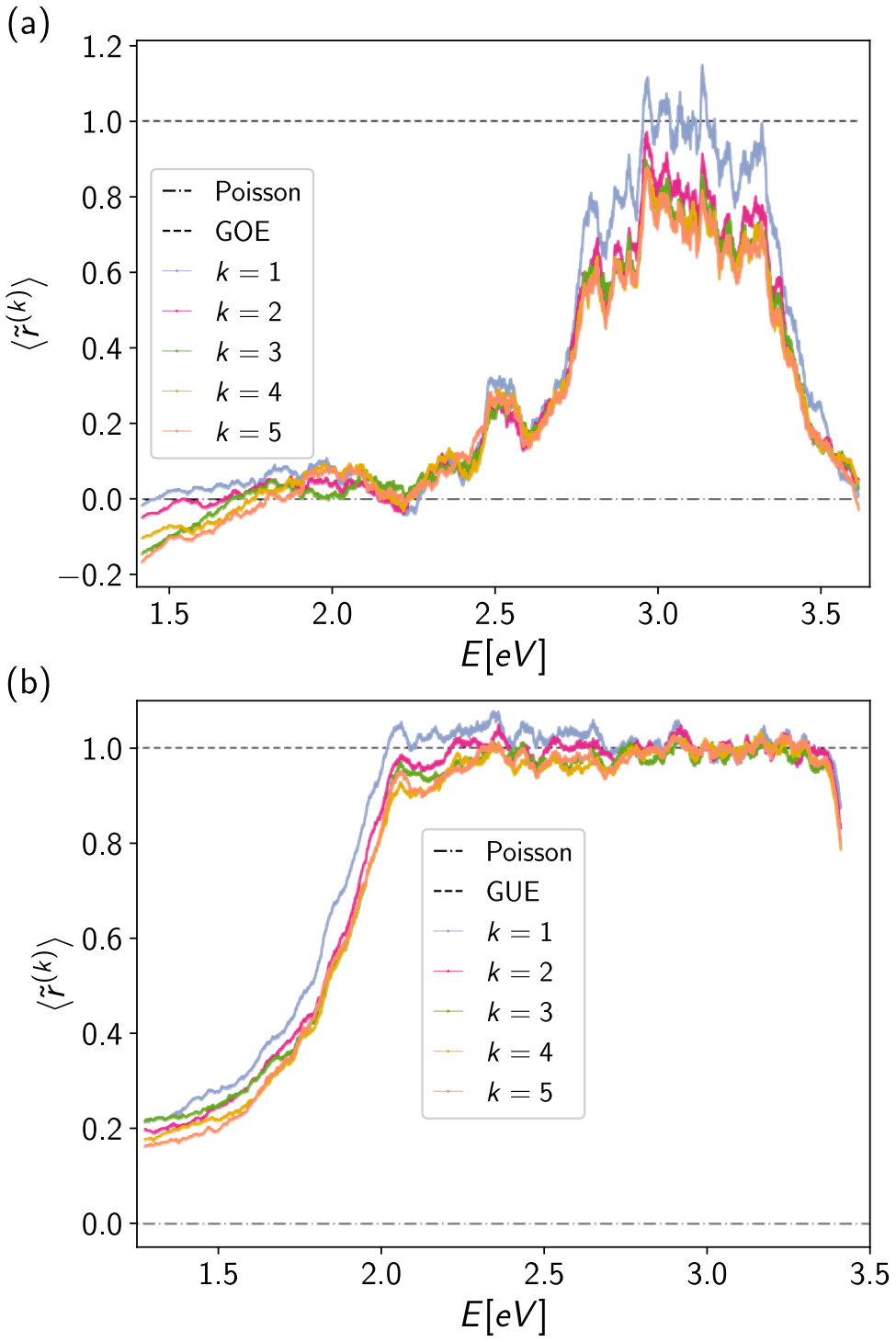

Fig. S5. Higher order reduced ratios presented as a function of the many-body energy for the (a) pristine [$\langle \tilde{r}(k) \rangle = 1$ represents the GOE universal result] and (b) lattice-disordered systems [$\langle \tilde{r}(k) \rangle = 1$ represents the GUE universal result].

[1] D. Hernangómez-Pérez, A. Kleiner, and S. Refaely-Abramson, Reduced absorption due to defect-localized interlayer excitons in transition-metal dichalcogenide–graphene heterostructures, Nano Lett. **23**, 5995 (2023).

[2] P. Giannozzi, S. Baroni, N. Bonini, M. Calandra, R. Car, C. Cavazzoni, D. Ceresoli, G. L. Chiarotti, M. Cococcioni, I. Dabo, A. Dal Corso, S. de Gironcoli, S. Fabris, G. Fratesi, R. Gebauer, U. Gerstmann, C. Gougoussis, A. Kokalj, M. Lazzeri, L. Martin-Samos, N. Marzari, F. Mauri, R. Mazzarello, S. Paolini, A. Pasquarello, L. Paulatto, C. Sbraccia, S. Scandolo, G. Sclauzero, A. P. Seitsonen, A. Smogunov, P. Umari, and R. M. Wentzcovitch, QUANTUM ESPRESSO: a modular and open-source software project for quantum simulations of materials, J. Phys. Condens. Matter **21**, 395502 (2009).

[3] P. Giannozzi, O. Andreussi, T. Brumme, O. Bunau, M. Buongiorno Nardelli, M. Calandra, R. Car, C. Cavazzoni, D. Ceresoli, M. Cococcioni, N. Colonna, I. Carnimeo, A. Dal Corso, S. de Gironcoli, P. Delugas, R. A. DiStasio, A. Ferretti, A. Floris, G. Fratesi, G. Fugallo, R. Gebauer, U. Gerstmann, F. Giustino, T. Gorni, J. Jia, M. Kawamura, H.-Y. Ko, A. Kokalj, E. Küçükbenli, M. Lazzeri, M. Marsili, N. Marzari, F. Mauri, N. L. Nguyen, H.-V. Nguyen, A. Otero-de-la Roza, L. Paulatto, S. Poncé, D. Rocca, R. Sabatini, B. Santra, M. Schlipf, A. P. Seitsonen, A. Smogunov, I. Timrov, T. Thonhauser, P. Umari, N. Vast, X. Wu, and S. Baroni, Advanced capabilities for materials modelling with Quantum ESPRESSO, J. Phys. Condens. Matter **29**, 465901 (2017).

[4] J. Deslippe, G. Samsonidze, D. A. Strubbe, M. Jain, M. L. Cohen, and S. G. Louie, BerkeleyGW: A massively parallel computer package for the calculation of the quasiparticle and optical properties of materials and nanostructures, Comput. Phys. Commun. **183**, 1269 (2012).

[5] M. Wu, *Spin-Orbit Coupling, Broken Time-Reversal Symmetry, and Polarizability Self-Consistency in GW and GW-BSE Theory with Applications to Two-Dimensional Materials*, Ph.D. thesis, University of California, Berkeley (2020).

[6] B. A. Barker, J. Deslippe, J. Lischner, M. Jain, O. V. Yazyev, D. A. Strubbe, and S. G. Louie, Spinor GW/Bethe-Salpeter calculations in BerkeleyGW: Implementation, symmetries, benchmarking, and performance, Phys. Rev. B **106**, 115127 (2022).

[7] V. Oganesyan and D. A. Huse, Localization of interacting fermions at high temperature, Phys.

Rev. B **75**, 155111 (2007).

[8] Y. Y. Atas, E. Bogomolny, O. Giraud, and G. Roux, Distribution of the ratio of consecutive level spacings in random matrix ensembles, Phys. Rev. Lett. **110**, 084101 (2013).

[9] S. H. Tekur, U. T. Bhosale, and M. S. Santhanam, Higher-order spacing ratios in random matrix theory and complex quantum systems, Phys. Rev. B **98**, 104305 (2018).

[10] W.-J. Rao, Higher-order level spacings in random matrix theory based on Wigner's conjecture, Phys. Rev. B **102**, 054202 (2020).

[11] I. Dumitriu and A. Edelman, Matrix models for beta ensembles, J. Math. Phys. **43**, 5830 (2002).